CLINICAL STUDY

Early response evaluation for recurrent high grade gliomas treated with bevacizumab: a volumetric analysis using diffusion-weighted imaging

Eui Jin Hwang · Yongjun Cha · A. Leum Lee · Tae Jin Yun · Tae Min Kim ·
Chul-Kee Park · Ji-Hoon Kim · Chul-Ho Sohn · Sung-Hye Park ·
Il Han Kim · Dae Seog Heo · Se-Hoon Lee · Seung Hong Choi

Abstract Bevacizumab is a novel treatment for the recurrent high-grade gliomas (rHGG). However, only a subset of the patients shows response to the bevacizumab treatment and the response evaluation using conventional criteria is difficult. The purpose of our study was to evaluate the early response for rHGG treated with bevacizumab using volumetric analysis of diffusion-weighted imaging (DWI). Twenty-nine patients who received bevacizumab therapy for rHGG were included in our study. All patients received a conventional MRI scan with DWI before and after the initial bevacizumab dose. For each MRI, we measured the total volume of the T2 hyperintense lesion (H_{T2}) of the rHGG, the volume of foci with a lower ADC value than that of the normal cortex (L_{ADC}), and the proportion of L_{ADC} to H_{T2} (L_{ADC}/H_{T2}). The Changes in the H_{T2}, L_{ADC} and L_{ADC}/H_{T2} after bevacizumab treatment were also determined. Thereafter, those volumetric data were compared to the progression free survival (PFS). After the analyses, we found a significant negative correlation between the PFS and the L_{ADC} for the post-bevacizumab ADC maps ($r = -0.413$, $P = 0.026$).

The patients with an L_{ADC} of <2.5 cm^3 showed a longer PFS than those with an L_{ADC} of ≥ 2.5 cm^3 (median = 135 vs. 91 days, $P = 0.002$) on the post-bevacizumab ADC maps. A multiple linear regression analysis revealed that only the post-bevacizumab L_{ADC} was a significant predictor of the PFS ($P = 0.026$). In conclusion, the post-bevacizumab L_{ADC} can be used for an early response evaluation and can predict the PFS for rHGG patients treated with bevacizumab.

Keywords Bevacizumab · Diffusion-weighted imaging · Glioblastoma · Astrocytoma · Prognosis

Introduction

Gliomas are the most common primary brain tumor, and the majority are high-grade gliomas (HGGs), including glioblastomas (GBMs) and anaplastic astrocytomas (AAs) [1, 2]. Despite recent advances in treatments, the clinical courses of patients with HGGs are grave and virtually every patient

E. J. Hwang · A. L. Lee · T. J. Yun · J.-H. Kim · C.-H. Sohn ·
S. H. Choi
Department of Radiology, Seoul National University College of
Medicine, 28, Yongon-dong, Chongno-gu, Seoul 110-744,
South Korea

Y. Cha · T. M. Kim · D. S. Heo · S.-H. Lee (✉)
Department of Internal Medicine, Cancer Research Institute,
Seoul National University College of Medicine, 28,
Yongon-dong, Chongno-gu, Seoul 110-744, South Korea
e-mail: shlee119@snu.ac.kr

C.-K. Park
Department of Neurosurgery, Seoul National University College
of Medicine, 28,
Yongon-dong, Chongno-gu, Seoul 110-744, South Korea

S.-H. Park
Department of Pathology, Seoul National University College of
Medicine, 28, Yongon-dong, Chongno-gu, Seoul 110-744,
South Korea

I. H. Kim
Department of Radiation Oncology, Cancer Research Institute,
Seoul National University College of Medicine, 28,
Yongon-dong, Chongno-gu, Seoul 110-744, South Korea

S. H. Choi (✉)
Center for Nanoparticle Research, Institute for Basic Science,
and School of Chemical and Biological Engineering,
Seoul National University, Seoul 151-742, Korea
e-mail: verocay@snuh.org

experiences a recurrence after the first line treatment [2, 3]. Bevacizumab, a humanized monoclonal antibody for the vascular endothelial growth factor (VEGF), has been shown to be effective for recurrent HGG (rHGG) as a single agent or in combination with chemotherapeutic agents such as irinotecan [2, 4–7]. The response rate for rHGG after treatment with bevacizumab has been reported to be 24.5–57.0 % [4, 5, 8, 9]. In spite of these encouraging results, a large subset of patients with rHGGs shows disease progression after the treatment. Furthermore, bevacizumab treatment induces restoration of the blood–brain barrier [2], which results in decreased contrast enhancement. Therefore, the conventional Macdonald criteria [10], which usually depend on contrast-enhanced imaging, become unreliable after bevacizumab treatment [11, 12]. Recently, the Response Assessment Neuro-Oncology (RANO) Working Group proposed new criteria for the tumor response assessment [12], which consider increasing T2 hyperintense lesion as an additional marker for tumor progression. However, the RANO criteria have some limitations in differentiating a true tumor infiltration from edema or gliosis [13]. Therefore, there have been enormous efforts to identify a new biomarker that can predict the treatment response or prognosis after treatment with bevacizumab for HGGs.

Diffusion-weighted image (DWI), which utilizes the Brownian motion of water molecules, has been shown to be able to provide information about cellular density and properties of the extracellular matrix [14]. Because extracellular water molecules move more freely than those in the intracellular spaces, the apparent diffusion coefficient (ADC) value calculated from DWI can serve as a marker of cellularity. This potential biomarker can be obtained without any radiation hazard or contrast media in only few minutes, and has been proven to be effective in predicting and monitoring the treatment of various cancers [15, 16]. Several recent studies have reported promising results for the prognosis evaluation of rHGG patients treated with bevacizumab using the ADC analysis of DWI [17–23]. However, most of the previous studies included patients treated with inhomogeneous chemotherapies or patients with heterogeneous pathologies (e.g., oligodendroglioma or mixed glioma). Therefore, the purpose of the present study was to evaluate the early response for rHGG with pure astrocytoma components following a treatment with bevacizumab and irinotecan using a volumetric analysis of DWI. In addition, we correlated the volumetric values from DWI with the progression free survival (PFS).

Materials and methods

Our institutional review board approved this study and informed consent was waived.

Patient selection

A total of 30 patients from our oncologic database were initially included for this retrospective study. Inclusion criteria were that each participant (a) had received pathologic diagnosis of GBM or AA with a World Health Organization grade of III or IV, respectively; (b) had started bevacizumab (Avastin, Genentech, South San Francisco, CA) therapy at our institute between October 2007 and May 2011; and (c) had been subjected to both baseline and follow up magnetic resonance imaging (MRI), including DWI, before and after the first dose of bevacizumab. Among those included patients, one patient who discontinued bevacizumab because of an economic problem without evidence of disease progression was excluded from the study. Consequently, 29 patients (20 male and 9 female patients; mean age of 51.2 years; 22 GBM and 7 AA) were analyzed.

Bevacizumab was administered as the second or third line chemotherapy, combined with topoisomerase inhibitor, irinotecan (Camptosar injection, Pfizer, New York, NY). The patients underwent initial craniotomy and tumor removal ($n = 16$) or stereotactic biopsy ($n = 13$). Postoperative radiation therapy, either concomitant chemoradiation therapy with temozolomide ($n = 11$) or radiation therapy alone ($n = 18$) was performed in all the patients. Bevacizumab was given every 2 weeks at our oncology day ward. After giving 125 mg/m^2 of irinotecan mixed with 200 ml of 5 % dextrose water over 90 min, 10 mg/kg of bevacizumab mixed with 100 ml of normal saline was administered intravenously over 60–90 min.

MRI acquisition

In each patient, a baseline MRI was performed before starting bevacizumab therapy (pre-bevacizumab MRI), and the first follow up MRI was also obtained (post-bevacizumab MRI). The mean time interval between the start of bevacizumab and the post-bevacizumab MRIs were 38.8 days (11–73 days). The pre- and post-bevacizumab MRI were performed using 1.5 T scanners [$n = 29$, Signa Excite 1.5T ($n = 18$); Signa HDxt 1.5T ($n = 8$); Signa HDx 1.5T ($n = 3$), GE Healthcare, Milwaukee, WI] or 3T scanners [$n = 29$, Verio ($n = 21$); Trio TIM ($n = 1$), Siemens Medical Solution, Erlangen, Germany; Signa Excite 3.0T, GE Healthcare, Milwaukee, WI ($n = 7$)]. The echo-planar DWIs were performed in the axial plane before the injection of the contrast material using b-values of 0 and 1,000 s/mm^2. The DWI was acquired in three orthogonal directions and combined into a trace image. Using these data, ADC maps were calculated on a voxel-by-voxel basis with the software incorporated into the MRI unit. In addition, MRIs included at least the axial

precontrast T1-weighted, T2-weighted fast spin-echo, and the fluid-attenuated inversion recovery T2-weighted images and contrast-enhanced axial T1-weighted images acquired after the contrast (Magnevist or Gadovist; Bayer Schering Pharma, Berlin, Germany; 0.1 mmol/kg) injection.

After the post-bevacizumab MRI, a follow up MRI was performed every 2–3 months or when the neurological symptoms were aggravated in the patients.

Image analysis

To quantify the tumor volume with the diffusion restriction, the areas on the ADC map corresponding to the T2 hyperintense lesions were first manually segmented by one author (S.H.C., 12-year-experience in neuroradiology). The segmentations of ADC map were performed for all the slices showing T2 hyperintensity. The identification of corresponding area with T2 hyperintensity on ADC map was performed by visual inspection, and then polygonal ROIs were placed on ADC maps for corresponding area with T2 hyperintensity. Drawing ROIs were performed with ImageJ software (Version 1.44p, 32 bit for Java 1.6.0, NIH, Bethesda, MD). After segmentation, the number of voxels in the segmented ROI and the ADC values of each voxel were calculated using our in-house program for each MRI. To minimize the bias due to various MR scanners, we used normalized ADC (nADC) value to define the foci with diffusion restriction in the tumor bed. The nADC value of each voxel was defined as ADC value of the voxel divided by the ADC value of normal cerebral cortex. The ADC values of the normal cortex were measured at the contralateral side of the main tumor, at the uppermost part of the brain. After deriving ADC value of segmented each segmented voxel and normal cerebral cortex, the numbers of voxels with nADC lesser than one, in other words, those with smaller ADC value than normal cerebral cortex were identified. By multiplying the number of voxel and the volume of each voxel, the total volume of the segmented T2 hyperintense lesion (H_{T2}) and the volume of the foci with nADC smaller than one (L_{ADC}) were calculated for each pre-bevacizumab and post-bevacizumab MRI. The proportions of the volume of foci with the nADC smaller than one to the volume of total T2 hyperintense tumor bed (L_{ADC}/H_{T2}) were also calculated. After the calculation of each volumetric data point in the pre- and post-bevacizumab MRI, the ratio of the post-bevacizumab volume data to the pre-bevacizumab volume data was calculated as a percentage for the interval changes of the H_{T2}, L_{ADC} and L_{ADC}/H_{T2} after the initial dose of bevacizumab using the following equation: interval change of each value = post-bevacizumab MRI value/pre-bevacizumab MRI value × 100.

Determination of tumor progression

The determination of the tumor progression was based on the response criteria developed by the RANO Working Group [12]. The patients who meet any one of following criteria were classified as progressive disease: (a) ≥ 25 % increase in sum of the products of perpendicular diameters of enhancing lesions with the smallest tumor measurement; (b) significant increase in T2/FLAIR nonenhancing lesion; (c) any new lesion; (d) clear clinical deterioration not attributable to other causes apart from the tumor; (e) failure to return for evaluation as a result of death or deteriorating condition; (f) clear progression of nonmeasurable disease. The PFS was calculated from the start of the bevacizumab and irinotecan therapy.

Statistical analysis

All the statistical analyses were performed with GraphPad InStat (Version 3.05, GraphPad Software, Inc., San Diego, CA) and PASW statistics (Version 18.0, SPSS Inc., Chicago, IL).

All of the variables were assessed for normality with a Kolmogorov–Smirnov test. A paired t test and Wilcoxon matched pairs test were used for comparing the volume data between the pre- and post-bevacizumab MRI. A Pearson's product-moment correlation test and a Spearman's Rank correlation test were used for assessing the correlation between the PFS and the volume data. The Kaplan–Meier method and Logrank test were used to assess the PFS. A stepwise multiple linear regression analysis was also performed to define the most important factor for predicting the PFS among those showing a significant correlation with the PFS. The results with P values less than 0.05 were considered statistically significant.

Results

Clinical outcome

All the patients showed disease progression during the follow up period, except for one patient who had an anaplastic astrocytoma involving the cerebellum. The median PFS was 121 days (25–442 days; 95 % confidence interval 107.81–134.19 days).

Among 28 patients with disease progression, 16 patients (57.1 %) showed progression of tumoral enhancement, while 8 patients (28.6 %) showed increased extent of T2 hyperintense lesion without progression of enhancing tumor lesion. The other 4 patients (14.3 %) were classified as progressive disease due to aggravation of neurologic status.
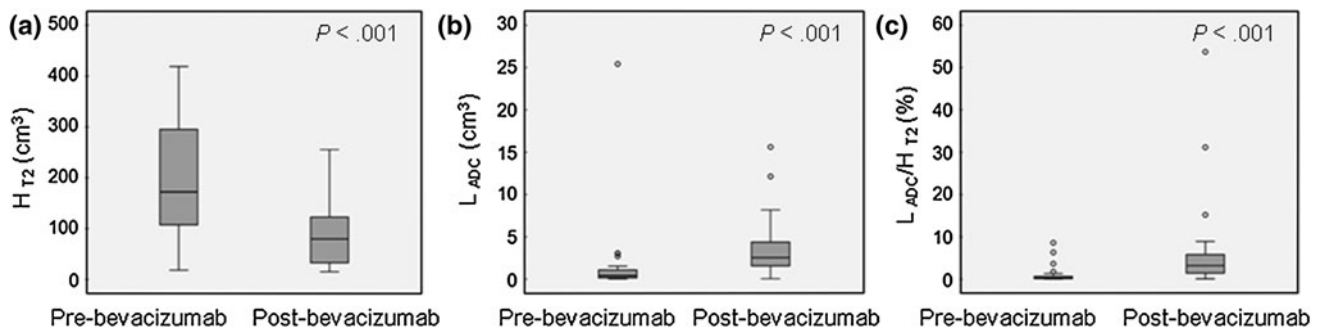
Fig. 1 The *box* and *whiskers plots* for the volumetric data in pre-bevacizumab and post-bevacizumab MRIs. The *whiskers* indicate the range of data, and the *boxes* represent the distance between the *first* and *third quartiles*, with the median value marked as a *line* in the *box*. The *asterisks* represent *outliers*. The volume of T2 hyperintense lesion (H_{T2}) showed a significant decrease (199.91 vs. 97.03 cm^3, $P < 0.001$) (**a**). The volume of the foci with a lower ADC value than the cortex (L_{ADC}) showed a significant increase (1.565 vs. 3.576 cm^3, $P < 0.001$) (**b**). The proportion of the L_{ADC} in the total H_{T2} (H_{T2}/L_{ADC}) showed a significant increase (0.96 vs. 6.37 %, $P < 0.001$) (**c**)

Patients' age did not showed significant correlation with PFS ($P = 0.580$ $r = -0.107$).

Change of volumetric data after initial dose of bevacizumab

Comparing pre- and post-bevacizumab MRI, there was a significant decrease in the H_{T2} after the initial bevacizumab dose (199.9 vs. 97.0 cm^3, $P < 0.001$), while the L_{ADC} showed a significant increase (1.6 vs. 3.6 cm^3, $P < 0.001$). The L_{ADC}/H_{T2} also showed a significant increase (1.0 vs. 6.4 %, $P < 0.001$). Figure 1 shows the box and whisker plots for the changes in volumetric data between the pre-bevacizumab and post-bevacizumab MRI.

Correlation between volumetric data and PFS

We performed correlation analyses on the PFS and the volumetric data acquired from the pre-bevacizumab and post-bevacizumab MRI. Figure 2 shows the results of correlation analyses. In brief, we found statistically significant negative correlations between the PFS and the L_{ADC} for the post-bevacizumab MRI ($P = 0.026$, $r = -0.413$) and between the PFS and the changes in the H_{T2} between the pre- and post- bevacizumab MRI ($P = 0.043$, $r = -0.378$). However, we could not find a significant correlation between the PFS and the other volumetric data.

Comparison of PFS according to clinical and volumetric data

A Kaplan–Meier survival analysis with a Logrank significance test was performed according to the patient gender, pathologic grade and type of surgery. We also performed a survival analysis for two MRI data including L_{ADC} for the post-bevacizumab MRI and the change in the H_{T2}, which were dichotomized into two groups. The results are summarized in Table 1 and Fig. 3. We found significant differences in the PFS, when dichotomized the patient group by L_{ADC} for the post-bevacizumab MRI (cutoff value = 2.5 cm^3) and by the change in H_{T2} between the pre- and post-bevacizumab MRI (cutoff value = 50 %). However, other factors, including gender, pathologic grade and surgery type did not show significant difference in PFS. The median PFS was significantly longer in the patients with L_{ADC} of <2.5 cm^3 ($n = 14$) compared with those patients with an L_{ADC} of ≥2.5 cm^3 ($n = 15$) (135 and 91 days, respectively, $P = 0.002$). There was a significantly longer median PFS in the patient group with the interval change of the H_{T2} of ≤50 % between pre- and post-bevacizumab MRI ($n = 14$) compared with the other group ($n = 15$) (129 and 85 days, respectively, $P = 0.011$).

Multiple regression analysis for PFS to find out most significant factor

Finally, a stepwise multiple linear regression analysis was performed using the PFS and the volumetric data showing significant correlation with PFS including the post-bevacizumab L_{ADC} and interval change of the H_{T2}. According to the result, the interval change of the H_{T2} was eliminated from the regression equation, and only the post-bevacizumab L_{ADC} was determined as a significant predictor of the PFS ($P = 0.026$).

Figure 4 shows the representative MRIs of a poor and a good responder to the bevacizumab and irinotecan treatment, respectively.

Discussion

In the present study, we observed a significant decrease in the H_{T2} after the initial bevacizumab dose, while both the L_{ADC} and L_{ADC}/H_{T2} showed significant increases. Furthermore,
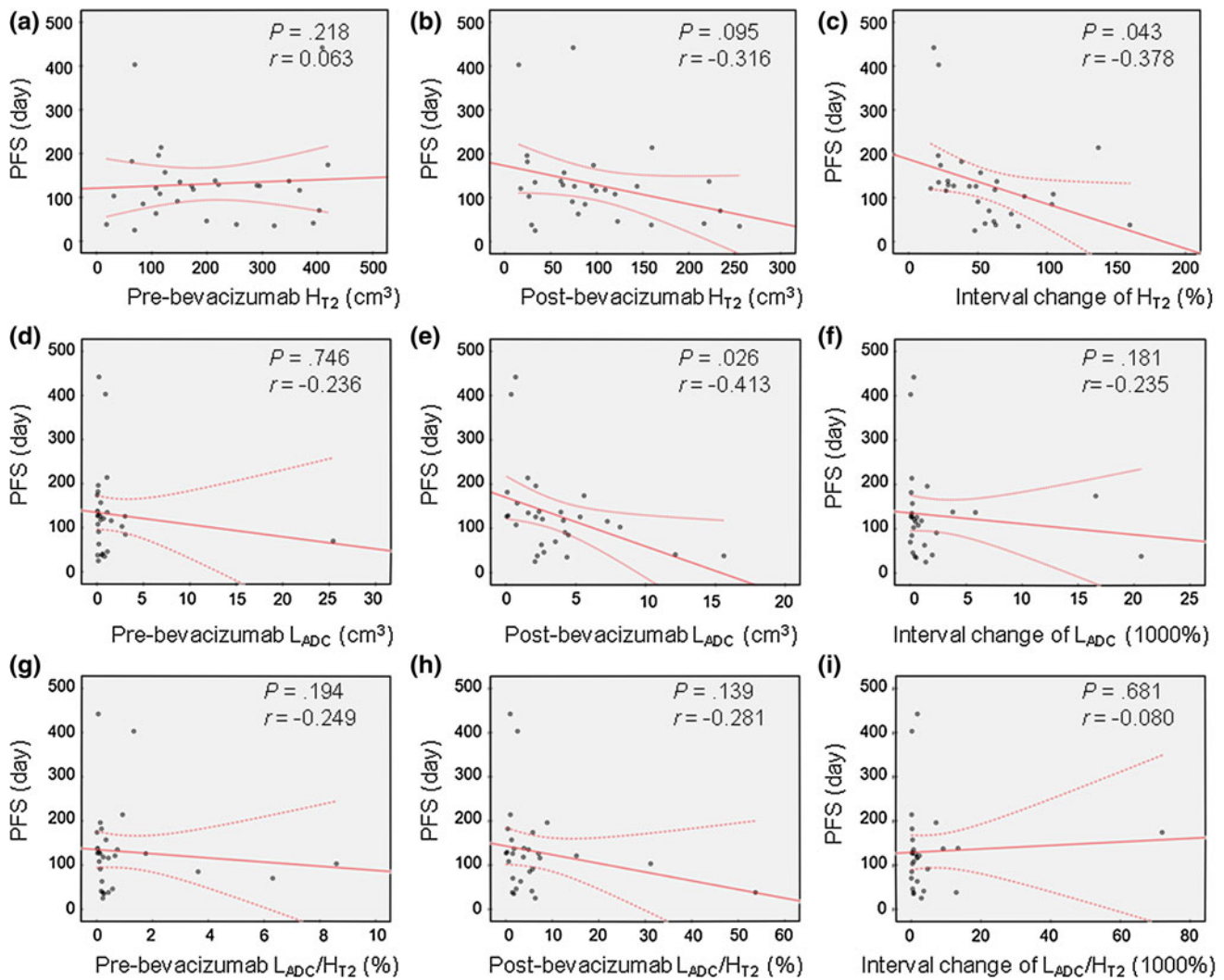
Fig. 2 The *scatter plots* showing the correlations between the PFS and the volumetric data. Only the interval change in the volume of the T2 hyperintense lesion (H_{T2}) after the initial dose of bevacizumab (Fig. 3c, $P = 0.043$, $r = -0.378$) and the volume of the foci with lower ADC value than the cortex (L_{ADC}) for the post-bevacizumab MRI (Fig. 3e, $P = 0.026$, $r = -0.413$) showed a significant negative correlation with the PFS, while the other volumetric data did not correlate significantly with the PFS. The *solid lines* indicate *trend lines* while *dashed lines* indicate the 95 % CI

we found significant negative correlations between the PFS and the L_{ADC} for the post-bevacizumab MRI ($P = 0.026$, $r = -0.413$), and between the PFS and the change in the H_{T2} between the pre- and post-bevacizumab MRI ($P = 0.043$, $r = -0.378$). In addition, the patients with an L_{ADC} of <2.5 cm^3 on the post-bevacizumab MRI or an interval change of ≤50 % in the H_{T2} showed longer PFS than the other patients. Among the volumetric values, the L_{ADC} for the post-bevacizumab MRI was the strongest predictor of the PFS in rHGG patients treated with bevacizumab and irinotecan.

T2 hyperintense lesions in rHGG patients indicate a heterogeneous pathologic nature that includes edema, ischemic changes, radiation effects and infiltrative tumor growth [13, 18]. Anti-angiogenic treatment induces a

reduction of cerebral edema by the elimination of VEGF and the restoration of the blood–brain barrier [2]. The decrease of the H_{T2} observed in our study can be explained by this "vascular-normalizing effect" of bevacizumab. In addition, we believe that a decreased tumor burden after the treatment also contributed to the shrinkage of the T2 hyperintense lesion. On the other hand, we also observed significant increases of L_{ADC} and L_{ADC}/H_{T2}. Persistent diffusion restriction in rHGG after an anti-angiogenic treatment has been reported in several studies, but the true pathologic nature of the diffusion restriction lesion in the tumor bed after bevacizumab treatment is still unclear. Gerstner et al. [24, 25] suggested the persistent diffusion restriction that occurs after anti-angiogenic therapy indicates an infiltrating tumor. On the other hand, Rieger et al. [23]

Table 1 Comparison of PFS according to clinical and volumetric data

	PFS (days)	P value[a]
Sex		0.158
Male ($n = 20$)	116 ± 11	
Female ($n = 9$)	138 ± 13	
Pathology		0.205
AA ($n = 7$)	118 ± 10	
GBM ($n = 22$)	129 ± 28	
Surgery		0.685
Biopsy ($n = 13$)	108 ± 18	
Tumor removal ($n = 16$)	121 ± 9	
Volume of foci with nADC <1 (L_{ADC}, cm^3) for the post-bevacizumab MRI		0.002
<2.5 cm^3 ($n = 14$)	135 ± 8	
≥2.5 cm^3 ($n = 15$)	91 ± 21	
Interval change in the volume of the hyperintense lesion (H_{T2})		0.011
≤50 % ($n = 14$)	129 ± 8	
>50 % ($n = 15$)	85 ± 18	

Except where indicated, the data are the median ± standard error

PFS progression free survival, *AA* anaplastic astrocytoma, *GBM* glioblastoma multiforme, *nADC* normalized apparent diffusion coefficient

[a] Logrank test

suggested that this persistent diffusion restriction may represent atypical necrosis and chronic hypoxia. Recently, Mong et al. [19] revealed a pathologically proven atypical necrosis in a lesion with persistent diffusion restriction in one patient. In terms of the T2 hyperintense lesions after treatment with bevacizumab, we believe diffusion restriction might indicate heterogeneous pathologic entities including residual tumors and treatment-related conditions.

On correlation analysis, only the post-bevacizumab L_{ADC} and the degree of the interval decrease of the H_{T2} showed significant correlation with the PFS. As mentioned above, we believe that a decrease of the H_{T2} is mainly due to a decrease of the edema. The residual H_{T2} after an initial dose of bevacizumab may represent the residual tumor volume after the elimination of the peritumoral edema. Therefore, a smaller decrease in the H_{T2} may mean the pre-bevacizumab H_{T2} was mainly composed of a true tumor volume. Consequently, this larger proportion of infiltrative tumor may explain the shorter PFS in the patients with less prominent shrinkage of the H_{T2}. Several studies have note T2 hyperintense lesions indicates an infiltrative tumor after anti-angiogenic treatment [2, 26]. In spite of multiple confounding factors such as edema or gliosis [13], a greater decrease in the H_{T2} after an initial bevacizumab dose can potentially be an early marker for a longer PFS. Although
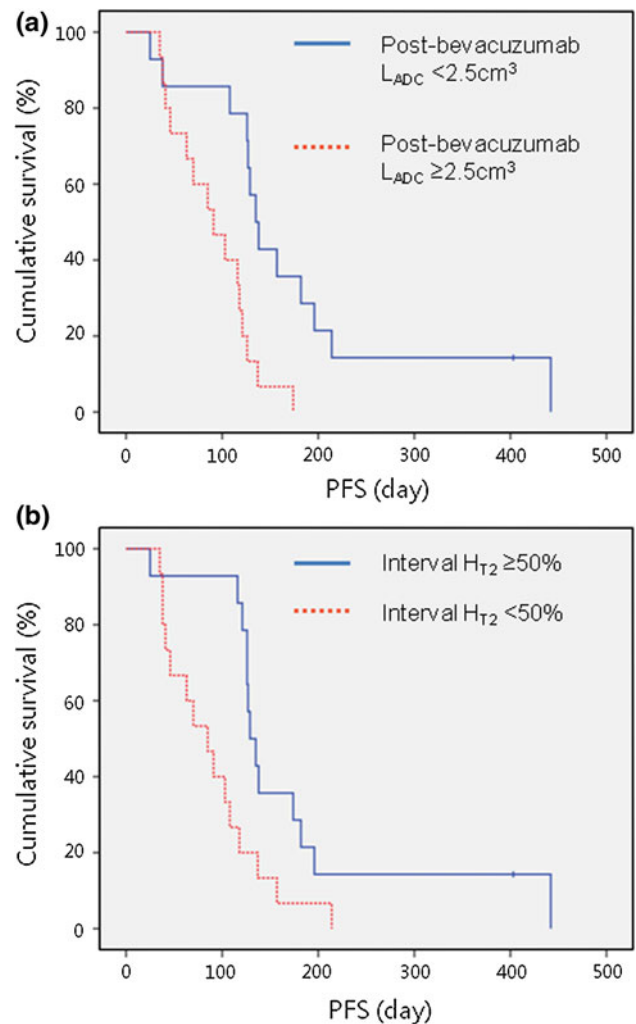

Fig. 3 The Kaplan–Meier curves for the PFS according to the volumetric data. The volume of the foci with a lower ADC value than the cortex (L_{ADC}) for the post-Bevacizumab MRI were classified as <2.5 versus ≥2.5 cm^3 (median PFS = 135 vs. 91 days, $P = 0.002$) (**a**). The changes in the volume of the T2 hyperintense lesion (H_{T2}) were classified as ≤50 versus >50 % (median PFS = 129 vs. 85 days, $P = 0.011$) (**b**)

we cannot exactly explain the pathologic entity of the lesion with diffusion restriction, we observed a significant correlation between PFS and post-bevacizumab L_{ADC}, which was also shown to be the only significant factor to predict the PFS on multiple regression analysis. This result supports the idea that persistent diffusion restriction is mainly ascribed to infiltrative tumors [24, 25]. There have been several studies in line with the present study. Jain et al. [18] reported progressive decrease in the ADC values both in enhancing and non-enhancing areas in patients with disease progression after bevacizumab administration. Nowosielski et al. [20] performed an ADC histogram analysis for T2 hyperintense lesions and showed increased histogram skewness after bevacizumab treatment, which is
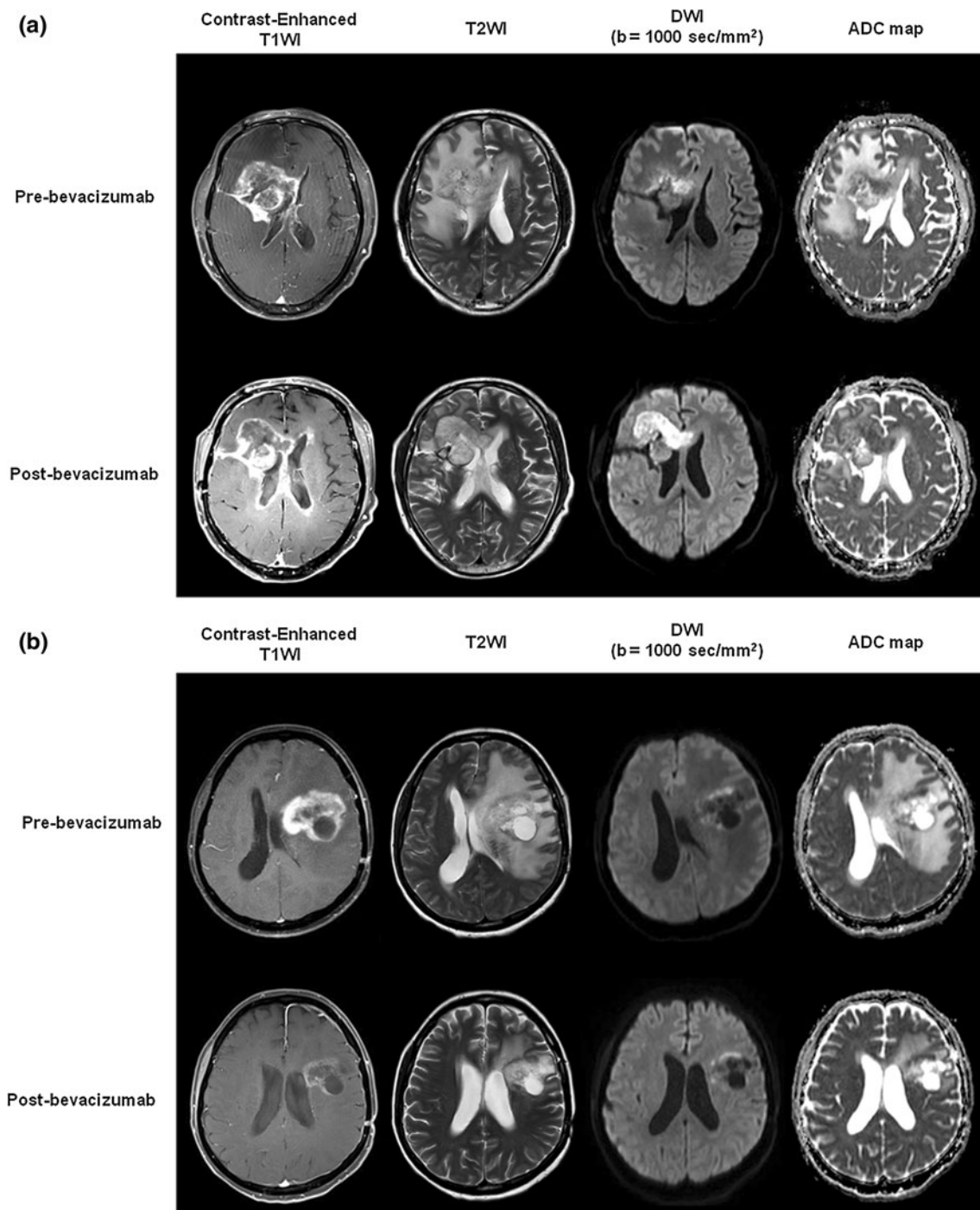
Fig. 4 a A case of a 58-year-old male with GBM showing a poor response to bevacizumab. After the initial dose of bevacizumab, the contrast enhancement and the T2 hyperintense lesion showed shrinkage. In contrast, the diffusion restriction foci increased in size. The PFS of the patient after bevacizumab treatment was 41 days. **b** A case of a 54-year-old female with GBM showing a good response to bevacizumab. After the initial dose of bevacizumab, the contrast enhancement and the T2 hyperintense lesion showed shrinkage. Meanwhile, the diffusion restriction foci did not change significantly. The PFS of the patient after bevacizumab treatment was 442 days

probably due to increased tumor cellularity in a portion, related to poor PFS. In addition, Ellingson et al. [17] suggested the functional diffusion map, made by mapping the changes in the ADC values and potentially reflects cellularity, as predictive biomarker for the anti-angiogenic treatment of malignant gliomas. In that study, hypercellular regions defined by the functional diffusion map were shown to be predictive of tumor progression. Mong et al. [19]

demonstrated better survival in patients with persistent diffusion restriction, which was explained by atypical necrosis. However, HGG shows a heterogeneous microstructure, and persistent diffusion restriction would not be explained by a single histopathologic nature. Considering the possible presence of atypical necrosis, we still believe that diffusion restriction is a useful marker for high cellularity because atypical necrosis after bevacizumab treatment is presumed to be the result of the pre-bevacizumab tumor infiltration.

Significantly longer PFS was observed in patients with an L_{ADC} of <2.5 cm^3 on the post-bevacizumab MRI than others. Although this threshold of 2.5 cm^3 derived from the present study requires further validation, the threshold can potentially be used in therapeutic decision making in individual patients. In patients with an L_{ADC} greater than 2.5 cm^3 on the post-bevacizumab MRI, thorough reconsideration for the continuation of bevacizumab treatment would be required.

The strong point of the present study, compared to previous studies based on diffusion-weighted imaging is that it is rather simple and straightforward, and therefore is more readily applicable in clinical practice. When the foci with diffusion restriction after bevacizumab treatment are larger, a shorter PFS would be expected. We included the patients with pure astrocytoma component, excluding patients with oligodendroglioma components, which show much favorable clinical course therefore cause a bias of the result. In addition, the present study only included patients who underwent combined treatment with bevacizumab and irinotecan, preventing the confounding caused by inhomogeneous therapeutic options.

Apart from the intrinsic limits of any retrospective study, several other limitations of our study should be mentioned. First, we used a variety of MRI scanners with different field strength (e.g., 1.5 and 3.0 T scanners) from different manufacturers, with scan parameters that were slightly different from each other. Not only the difference of main magnetic field strength but also differences of scan parameters and processing methodologies of DWIs can cause some biases on ADC measurement. However, Chawla et al. [27] have reviewed previous reports and suggested that ADC is a field-strength-independent parameter. Furthermore, we normalized the ADC values using the ADC values of the cerebral cortex to minimize the potential bias. Second, there were only a small number of patients who met the inclusion criteria. A multi-center based study with a larger group of patients may solve this problem in the future. Third, the post-bevacizumab MRIs were not obtained regularly and the intervals between the post-bevacizumab MRI and initial bevacizumab dose ranged from 11 to 73 days (mean time interval 38.8 days; standard deviation 11.1 days). This variation might be one

of biases, because the effect of bevacizumab on blood–brain barrier would vary according to cumulative dose and duration of administration. However, the majority of the intervals were approximately 40 days (79.3 % of patients between 30 and 50 days), so we believe that the bias due to the various follow up intervals did not significantly affect the results. In addition, we would like to recommend the 4–5 weeks follow-up MRI with DWI for the early response evaluation to bevacizumab in high grade glioma patients for the future study. Fourth, the segmentation of ADC maps was manually performed by visual inspection of both T2WI and ADC maps, which might result in a bias due to the poor delineation of T2 hyperintensity in some cases. However, we could minimize the difference between each case for the analysis of both T2 hyperintensity and ADC maps by the meticulous evaluation. Probably, the automatic or semiautomatic segmentation with co-registration of T2WI and ADC map can be a solution for these limitations, which warranted in the future study. In addition, the reproducibility of the segmentation method has not been addressed, which is also need to be validated in the future study.

In conclusion, post-bevacizumab DWI can serve as an imaging marker for the early treatment response and can predict the PFS for patients with rHGG after bevacizumab treatment. In particular, the volume of the foci with lower ADC value than the normal cerebral cortex in the tumor bed of after an initial dose of bevacizumab can be predictive for PFS after bevacizumab treatment. We believe DWI, which can be performed in a relatively short exam time and without contrast media, would become an important imaging technique in evaluating rHGG after bevacizumab treatment.

References

1. Behin A, Hoang-Xuan K, Carpentier AF, Delattre JY (2003) Primary brain tumours in adults. Lancet 361:323–331
2. Norden AD, Drappatz J, Wen PY (2008) Novel anti-angiogenic therapies for malignant gliomas. Lancet Neurol 7:1152–1160
3. Lamborn KR, Yung WK, Chang SM, Wen PY, Cloughesy TF, DeAngelis LM, Robins HI, Lieberman FS, Fine HA, Fink KL, Junck L, Abrey L, Gilbert MR, Mehta M, Kuhn JG, Aldape KD, Hibberts J, Peterson PM, Prados MD (2008) Progression-free survival: an important end point in evaluating therapy for recurrent high-grade gliomas. Neuro Oncol 10:162–170

4. Chamberlain MC (2011) Bevacizumab for the treatment of recurrent glioblastoma. Clin Med Insights Oncol 5:117–129

5. de Groot JF, Yung WK (2008) Bevacizumab and irinotecan in the treatment of recurrent malignant gliomas. Cancer J 14:279–285

6. Vredenburgh JJ, Desjardins A, Herndon JE 2nd, Dowell JM, Reardon DA, Quinn JA, Rich JN, Sathornsumetee S, Gururangan S, Wagner M, Bigner DD, Friedman AH, Friedman HS (2007) Phase II trial of bevacizumab and irinotecan in recurrent malignant glioma. Clin Cancer Res 13:1253–1259

7. Vredenburgh JJ, Desjardins A, Herndon JE 2nd, Marcello J, Reardon DA, Quinn JA, Rich JN, Sathornsumetee S, Gururangan S, Sampson J, Wagner M, Bailey L, Bigner DD, Friedman AH, Friedman HS (2007) Bevacizumab plus irinotecan in recurrent glioblastoma multiforme. J Clin Oncol 25:4722–4729

8. Friedman HS, Prados MD, Wen PY, Mikkelsen T, Schiff D, Abrey LE, Yung WK, Paleologos N, Nicholas MK, Jensen R, Vredenburgh J, Huang J, Zheng M, Cloughesy T (2009) Bevacizumab alone and in combination with irinotecan in recurrent glioblastoma. J Clin Oncol 27:4733–4740

9. Kreisl TN, Kim L, Moore K, Duic P, Royce C, Stroud I, Garren N, Mackey M, Butman JA, Camphausen K, Park J, Albert PS, Fine HA (2009) Phase II trial of single-agent bevacizumab followed by bevacizumab plus irinotecan at tumor progression in recurrent glioblastoma. J Clin Oncol 27:740–745

10. Macdonald DR, Cascino TL, Schold SC Jr, Cairncross JG (1990) Response criteria for phase II studies of supratentorial malignant glioma. J Clin Oncol 8:1277–1280

11. Sorensen AG, Batchelor TT, Wen PY, Zhang WT, Jain RK (2008) Response criteria for glioma. Nat Clin Pract Oncol 5:634–644

12. Wen PY, Macdonald DR, Reardon DA, Cloughesy TF, Sorensen AG, Galanis E, Degroot J, Wick W, Gilbert MR, Lassman AB, Tsien C, Mikkelsen T, Wong ET, Chamberlain MC, Stupp R, Lamborn KR, Vogelbaum MA, van den Bent MJ, Chang SM (2010) Updated response assessment criteria for high-grade gliomas: response assessment in neuro-oncology working group. J Clin Oncol 28:1963–1972

13. Pope WB, Young JR, Ellingson BM (2011) Advances in MRI assessment of gliomas and response to anti-VEGF therapy. Curr Neurol Neurosci Rep 11:336–344

14. Charles-Edwards EM, de Souza NM (2006) Diffusion-weighted magnetic resonance imaging and its application to cancer. Cancer imaging 6:135–143

15. Padhani AR, Liu G, Koh DM, Chenevert TL, Thoeny HC, Takahara T, Dzik-Jurasz A, Ross BD, Van Cauteren M, Collins D, Hammoud DA, Rustin GJ, Taouli B, Choyke PL (2009) Diffusion-weighted magnetic resonance imaging as a cancer biomarker: consensus and recommendations. Neoplasia 11:102–125

16. Thoeny HC, Ross BD (2010) Predicting and monitoring cancer treatment response with diffusion-weighted MRI. J Magn Reson Imaging 32:2–16

17. Ellingson BM, Malkin MG, Rand SD, LaViolette PS, Connelly JM, Mueller WM, Schmainda KM (2011) Volumetric analysis of functional diffusion maps is a predictive imaging biomarker for cytotoxic and anti-angiogenic treatments in malignant gliomas. J Neurooncol 102:95–103

18. Jain R, Scarpace LM, Ellika S, Torcuator R, Schultz LR, Hearshen D, Mikkelsen T (2010) Imaging response criteria for recurrent gliomas treated with bevacizumab: role of diffusion weighted imaging as an imaging biomarker. J Neurooncol 96:423–431

19. Mong S, Ellingson BM, Nghiemphu PL, Kim HJ, Mirsadraei L, Lai A, Yong W, Zaw TM, Cloughesy TF, Pope WB (2012) Persistent diffusion-restricted lesions in bevacizumab-treated malignant gliomas are associated with improved survival compared with matched controls. AJNR Am J Neuroradiol 33(9):1763–1770

20. Nowosielski M, Recheis W, Goebel G, Guler O, Tinkhauser G, Kostron H, Schocke M, Gotwald T, Stockhammer G, Hutterer M (2011) ADC histograms predict response to anti-angiogenic therapy in patients with recurrent high-grade glioma. Neuroradiology 53:291–302

21. Pope WB, Kim HJ, Huo J, Alger J, Brown MS, Gjertson D, Sai V, Young JR, Tekchandani L, Cloughesy T, Mischel PS, Lai A, Nghiemphu P, Rahmanuddin S, Goldin J (2009) Recurrent glioblastoma multiforme: ADC histogram analysis predicts response to bevacizumab treatment. Radiology 252:182–189

22. Pope WB, Qiao XJ, Kim HJ, Lai A, Nghiemphu P, Xue X, Ellingson BM, Schiff D, Aregawi D, Cha S, Puduvalli VK, Wu J, Yung WK, Young GS, Vredenburgh J, Barboriak D, Abrey LE, Mikkelsen T, Jain R, Paleologos NA, Rn PL, Prados M, Goldin J, Wen PY, Cloughesy T (2012) Apparent diffusion coefficient histogram analysis stratifies progression-free and overall survival in patients with recurrent GBM treated with bevacizumab: a multi-center study. J Neurooncol 108:491–498

23. Rieger J, Bahr O, Muller K, Franz K, Steinbach J, Hattingen E (2010) Bevacizumab-induced diffusion-restricted lesions in malignant glioma patients. J Neurooncol 99:49–56

24. Norden AD, Young GS, Setayesh K, Muzikansky A, Klufas R, Ross GL, Ciampa AS, Ebbeling LG, Levy B, Drappatz J, Kesari S, Wen PY (2008) Bevacizumab for recurrent malignant gliomas: efficacy, toxicity, and patterns of recurrence. Neurology 70:779–787

25. Gerstner ER, Chen PJ, Wen PY, Jain RK, Batchelor TT, Sorensen G (2010) Infiltrative patterns of glioblastoma spread detected via diffusion MRI after treatment with cediranib. Neuro Oncol 12:466–472

26. Gerstner ER, Frosch MP, Batchelor TT (2010) Diffusion magnetic resonance imaging detects pathologically confirmed, non-enhancing tumor progression in a patient with recurrent glioblastoma receiving bevacizumab. J Clin Oncol 28:e91–e93

27. Chawla S, Kim S, Wang S, Poptani H (2009) Diffusion-weighted imaging in head and neck cancers. Future Oncol 5:959–975